# Mannose 6-phosphate receptors, Niemann-Pick C2 protein, and lysosomal cholesterol accumulation

**Marion Willenborg,* Christine Kathrin Schmidt,* Peter Braun,† Jobst Landgrebe,† Kurt von Figura,† Paul Saftig,[1,*] and Eeva-Liisa Eskelinen[1,2,*,§]**

Institute of Biochemistry,* University of Kiel, D-24098 Kiel, Germany; Institute of Biochemistry 2,† University of Göttingen, D-37075 Göttingen, Germany; and Division of Biochemistry,§ Department of Biological and Environmental Sciences, FI-00014 University of Helsinki, Helsinki, Finland

**Abstract** **Niemann-Pick disease type C (NPC), caused by mutations in the *NPC1* gene or the *NPC2* gene, is characterized by the accumulation of unesterified cholesterol and other lipids in endo/lysosomal compartments. NPC2 is a small, soluble, lysosomal protein that is targeted to this compartment via a mannose 6-phosphate-inhibitable pathway. To obtain insight into the roles of mannose 6-phosphate receptors (MPRs) in NPC2 targeting, we here examine the trafficking and function of NPC2 in fibroblast lines deficient in one or both of the two MPRs, MPR46 and MPR300. We demonstrate that either MPR alone is sufficient to transport NPC2 to the endo/lysosomal compartment, although MPR300 seems to be more efficient than MPR46. In the absence of both MPRs, NPC2 is secreted into the culture medium, and only a small amount of intracellular NPC2 can be detected, mainly in the endoplasmic reticulum. This leads to massive accumulation of unesterified cholesterol in the endo/lysosomal compartment of the MPR46/300-deficient fibroblasts, a phenotype similar to that of the NPC patient fibroblasts. In addition, we observed an upregulation of NPC1 protein and mRNA in the MPR-double-deficient cells. Taken together, our results suggest that the lysosomal targeting of NPC2 is strictly dependent on MPRs in fibroblasts.**—Willenborg, M., C. K. Schmidt, P. Braun, J. Landgrebe, K. von Figura, P. Saftig, and E-L. Eskelinen. **Mannose 6-phosphate receptors, Niemann-Pick C2 protein, and lysosomal cholesterol accumulation.** ***J. Lipid Res.*** **2005.** 46: **2559–2569.**

**Supplementary key words** NPC1 • NPC2 • cholesterol • late endosome

Niemann-Pick C (NPC) disease is an autosomally inherited neurovisceral lipid storage disease caused by mutations in the *NPC1* gene or the *NPC2* gene (1). The disease is characterized by the accumulation of unesterified cholesterol, derived from endocytosed LDL, glycolipids (sphingomyelin, glucosyl- and lactosylceramide, and gangliosides GM2 and GM3), and bis(monoacylglycero)phosphate/lysobisphosphatidic acid, in late endosomes or lysosomes of many tissues, including fibroblasts. LDL-induced cholesterol esterification and LDL-mediated suppression of cholesterol synthesis are also impaired (2). The majority (95%) of patients have mutations in the *NPC1* gene, which encodes a large membrane protein with 13 transmembrane domains, located in late endosomes (3). The remainder of patients have mutations in the *NPC2* gene, which encodes a small, soluble, lysosomal protein (4). NPC1 has been proposed to act as a transmembrane pump for unidentified lipids (5). NPC1 binds cholesterol, but with a low affinity (6). NPC2 binds cholesterol with high affinity, and this binding activity is necessary for its control of lysosomal cholesterol levels (7). The precise functions of NPC1 and NPC2, however, remain unclear and are currently under intense investigation. Mice deficient in NPC1, hypomorphous in NPC2, and crosses of these two genotypes have been generated. The phenotype of the NPC1 single-mutant mice is very similar to the phenotype of the double-mutant mice (8). This and other results support the idea that the NPC1 and NPC2 proteins function at two different steps of the same pathway that transports cholesterol and other lipids out of late endosomes and/or lysosomes (1). It has been proposed that NPC2 binds cholesterol from the internal lysosomal/late-endosomal membranes, and thus enables the physical interaction of cholesterol with NPC1 or another protein (2). However, it has been shown that NPC1 can bind cholesterol in cells that lack the NPC2 protein (6), indicating that this interaction is not dependent on NPC2 function.

The role of the NPC2 protein in NPC disease was discovered only recently. Unexpectedly, NPC2 was found to

Abbreviations: BMP, bis(monoacylglycero)phosphate; endo H, endoglycosidase H; ER, endoplasmic reticulum; MEF, mouse embryonic fibroblast; MPR, mannose 6-phosphate receptor; NPC, Niemann-Pick type C; PNGase F, peptide *N*-glycosidase F; TGN, trans Golgi network.

[1] P. Saftig and E-L. Eskelinen contributed equally to this work.
[2] To whom correspondence should be addressed.
e-mail Eeva-Liisa.Eskelinen@Helsinki.Fi

*Manuscript received 5 April 2005 and in revised form 29 August 2005.*
*Published, JLR Papers in Press, September 21, 2005.*
*DOI 10.1194/jlr.M500131-JLR200*

be a secretory protein in many tissues (4, 9). NPC2, however, contains the lysosomal mannose 6-phosphate tag, and accordingly, NPC2 also localizes in the lysosomal compartment (4, 10). Thus, it is likely that NPC2 needs mannose 6-phosphate receptors (MPRs; see below) for lysosomal targeting.

Soluble lysosomal enzymes or proteins are targeted to the lysosomal compartments by MPRs that bind to the mannose 6-phosphate tags on the newly synthesized enzymes in the trans Golgi network (TGN) (11). Two MPRs exist: the 46 kDa (cation-dependent) receptor and the 300 kDa (cation-independent) receptor. Both MPRs are necessary for efficient lysosomal targeting of newly synthesized enzymes, suggesting that the two MPRs have complementary targeting functions, possibly by binding to different features on the mannose 6-phosphate ligands (12–14).

When NPC2 patient fibroblasts were fed with medium from cells producing wild-type NPC2, the cholesterol storage phenotype of the NPC2 cells was cured (4, 7, 15). Addition of mannose 6-phosphate to the culture medium prevented this rescue effect (4), suggesting that the uptake was dependent on MPRs. The aim of this study was to investigate the roles of the two MPRs, MPR46 and MPR300, in the targeting of NPC2 to the lysosomal compartment. We also characterized the effects of NPC2 mistargeting on the level of NPC1 protein, as well as on cholesterol accumulation, in fibroblast cell lines deficient in MPR46, MPR300, or both MPRs.

## MATERIALS AND METHODS

### Cell lines and mice

Mouse embryonic fibroblasts (MEFs) deficient in MPR46, MPR300, or both MPRs have been described previously (14). The cells were immortalized using the Simian virus 40 large T antigen. DMEM containing 10% fetal calf serum and penicillin-streptomycin was used to culture the cells.

### Antibodies

The following primary antibodies were used: rabbit anti-MPR46 MSC1, mouse anti-human MPR46 (10C6) (16), rabbit anti-rat MPR300 (17), goat anti-human MPR300 (made in the laboratory of Kurt von Figura), rat anti-mouse LAMP-1 (1D4B, Developmental Studies Hybridoma Bank; Iowa City, IA), rabbit anti-mouse NPC1 (a gift of Wiliam Garver), rabbit antibody against recombinant human NPC2 (a gift of Shutish Patel), mouse anti-syntaxin 6 (BD Transduction Laboratories; Heidelberg, Germany), a mouse antibody against protein disulphide isomerase (1D3, a gift of Stephen Fuller), mouse anti-tubulin (E7, Developmental Studies Hybridoma Bank), mouse anti-LBPA/BMP (a gift of Jean Gruenberg), mouse anti-*N*-cadherin (BD Transduction Laboratories), and rabbit anti-GM2 (Acris Antibodies; Hiddenhausen, Germany).

### Plasmids, transfection

Human MPR46 in pBHE2222 (18) and human MPR300 in pCIneo (19) were gifts of Thomas Braulke. Dog Rab7 in pEGFP-C1 was a gift of Cecilia Bucci (20). The cells were transiently transfected using Fugene 6 (Roche; Mannheim, Germany) according to the manufacturer's instructions.

### Immunofluorescence staining

The cells were grown on glass coverslips, fixed in 4% paraformaldehyde in phosphate-buffered saline (PBS) for 30 min, and permeabilized with 0.1% Triton X-100. For immunostaining of endogenous NPC2, the cells were fixed in Bouin's solution (picric acid-formalin-acetic acid; 15:5:1) for 1 h. The primary and secondary antibodies were diluted in 3% BSA and incubated on the cells for 1 h. Alexa Fluor 350-, 488-, or 594-conjugated secondary antibodies were from Molecular Probes (Eugene, OR). Finally, the cells were embedded in Mowiol containing triethylenediamine as an antifading agent. Filipin staining (0.5 mg/ml in PBS for 1 h) was performed before immunolabeling. In these experiments, no further permeabilzation was performed. The samples were examined and photographed with a Zeiss Axiovert 200M fluorescence microscope equipped with an Apotome to generate optical sections and an Axiocam MRm Rev. 2D camera, using Axiovision Software Rel 4.2 (Zeiss; Göttingen, Germany).

### Electron microscopy

Cells were grown on plastic dishes and fixed in 2% glutaraldehyde in 0.2 M Hepes, pH 7.4, for 15 min. Filipin (0.5 mg/ml) was then added to the fixative, and the incubation was continued for 2 h with gentle agitation. The cell monolayers were postfixed in 1% osmium tetroxide, stained with 3% uranyl acetate, and flat-embedded in Agar 100 resin using standard procedures. Thin sections were cut, stained with uranyl acetate and lead citrate, and examined using a Zeiss 900 transmission electron microscope.

### Western blotting

Cell or tissue extracts were prepared using PBS, 2% NP-40, 0.2% SDS, and a proteinase inhibitor cocktail (Roche; Grenzach, Germany). For NPC2 protein, 15% SDS-PAGE gels or 4–12% NuPAGE gels (Invitrogen; Karlsruhe, Germany) were used. Proteins were transferred to polyvinylidene difluoride membranes using a semidry blotting system. Skimmed milk powder (5%) in TBS with 0.01% Tween 20 was used for blocking. Donkey anti-rabbit horseradish peroxidase (Santa Cruz Biotechnology Ltd., Santa Cruz, CA ) was used as a secondary antibody. Signals were detected using the ECL Super Western Blotting Detection System or ECL Advance Western Blotting Detection Kit (Amersham; Freiburg, Germany). After immunostaining and ECL detection, the blots were stained with Ponceau protein stain to test protein loading and even transfer to the blotting membrane. In some experiments, the blots were then stripped and immunostained using anti-tubulin or anti-*N*-cadherin to check the protein loading and transfer.

### Enzyme digestion with peptide *N*-glycosidase F (PNGase F) and endoglycosidase H (endo H)

PNGase F and endo H were from Roche (Mannheim, Germany). For PNGase F digestion, the proteins of cell extracts were denatured in 50 mM $Na_3PO_4$ buffer, pH 7.8, containing 1% SDS, 1% 2-mercaptoethanol, and proteinase inhibitor cocktail, for 5 min at 100°C. Digestion was performed in 50 mM trisodium phosphate buffer, pH 7.5, containing 0.1% SDS, 0.1% 2-mercaptoethanol, 1% NP-40, and proteinase inhibitor cocktail. One unit of PNGase F was used for 20 μg protein, and the digestion was carried out for 3 h at 37°C. For endo H digestion, the denaturation and digestion were carried out in 100 mM sodium citrate buffer, pH 5.5, containing 0.5 M sodium rhodanid, 0.1% 2-mercaptoethanol, and 1% SDS. For 25 μg of protein, 6.35 mU of endo H was used, and the digestion was performed overnight at 37°C.

### Cholesterol assay

Total cholesterol levels were determined using Amplex Red cholesterol assay kit (Molecular Probes) as described (21).

### Northern blotting

Total RNA of fibroblasts was prepared using phenol-chloroform extraction. Total RNA samples (5, 10, and 15 μg) were separated in a formaldehyde agarose gel and processed as described (22). Filters were hybridized with an NPC1 or NPC2 cDNA probe. Hybridzation and washing steps were performed as described (23). Hybridization with an actin cDNA probe was used as loading control.

### Lipid preparation and thin-layer chromatography (TLC) analysis

For each cell line, lipids from five 10 cm dishes were extracted according to the method of Folch, Lees, and Sloane (24) and dissolved in 1 ml *N*-hexane. For the TLC, silica gel (F254) high-performance TLC plates were prerun in chloroform-methanol (1:1), heated at 110°C, cooled at room temperature, and loaded with standards and 10 μl of the prepared lipid samples. The plates were run in methylacetate-*N*-propanol-chloroform-methanole-potassium chloride 0.25% (w/v in water), 25:25:28:10:7. The plates were then dried and sprayed extensively with 10% copper sulfate (w/v in 8% orthophosphoric acid). The lipids were charred at 180°C for 12 min.

## RESULTS

### Mouse NPC2 is mistargeted to the medium in fibroblasts deficient in MPRs

MEF lines deficient in MPR46, MPR300, or both, as well as control cells, were used in this study. To verify the genotypes, the cell lines were examined by immunofluorescence microscopy using MPR46 and MPR300 antibodies (**Fig. 1**).

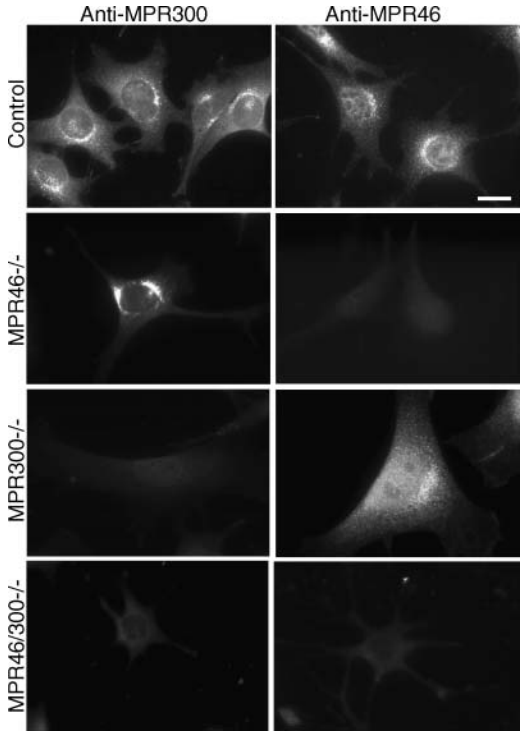


**Fig. 1.** Immunofluorescence staining of endogenous MPR46 and MPR300 in mouse fibroblast lines. The genotype of the cell lines is indicated at left. Bar = 10 μm.

NPC2 is a soluble protein that contains a mannose 6-phosphate tag (4). Glycosylation of Asn58 was shown to be necessary for lysosomal targeting of the human NPC2 (15). Thus, it is likely that NPC2 needs MPRs for lysosomal targeting. We performed Western blotting to investigate the intracellular retention of NPC2 protein in our MPR-deficient cell lines. In control cell extracts, we detected two bands at approximately 18 kDa and 16 kDa (**Fig. 2A**), in agreement with published results (4, 9). These two forms have been suggested to represent glycosylation variants. The bands of MPR46$^{-/-}$ cells were similar to those of control cells; however, the intensity of the 16 kDa band was slightly lower than in control cells. In MPR300$^{-/-}$ cells, the 16 kDa band was slightly shifted to a form with a higher molecular mass. In addition, the intensity of this band was again lower than in the control cells or in MPR46$^{-/-}$ cells. In MPR-double-deficient cells, the 16 kDa band was absent, whereas the 18 kDa band was still detectable. Quantitation of the band intensities is presented in Fig. 2B. Taken together, the Western blotting results indicate that although both MPRs are necessary for maximal intracellular retention of NPC2, either MPR alone is able to mediate a substantial intracellular retention. However, MPR300 may be slightly more efficient in intracellular targeting than MPR46.

Low intracellular levels of NPC2 in the MPR-double-deficient cells suggested that more NPC2 might be secreted into the culture medium. To investigate this, we performed Western blotting of the culture medium. As expected, we could detect NPC2 in the culture medium of the MPR-double-deficient cells (Fig. 2C). Only trace amounts of NPC2 were detected in the culture medium of control cells or the MPR-single-deficient cells, suggesting that either receptor alone was able to mediate intracellular retention and to target NPC2 to the lysosomal compartment. This result is in agreement with the quantitative Western blotting of intracellular NPC2 (Fig. 2A, B).

### Complex-type carbohydrates are not linked to NPC2 in MPR300-deficient fibroblasts

Lysosomal and secretory proteins are initially glycosylated in the endoplasmic reticulum (ER). The Golgi enzymes further modify the added carbohydrate chains once the protein is transported from the ER to the Golgi. *N*-glycosylated proteins are sensitive for endo H enzyme unless their carbohydrate chains are modified by enzymes localized in the mid-Golgi region to complex-type oligosaccharides (25). However, all *N*-glycosylated proteins are sensitive to PNGase F digestion (26). PNGase F cleaves off all *N*-linked carbohydrate chains, leaving behind the polypeptide with possible attached O-linked sugar chains. We used these two glycosidases to investigate the glycosylation of NPC2 in our cell lines. The mouse NPC2 protein has three potential *N*-glycosylation sites: Asn 38, Asn58, and Asn69. Lysosomal targeting of human NPC2 was found to depend on glycosylation of Asn58, which is located in a region conserved in NPC2 orthologs (15). PNGase treatment of the cell extract of our cells produced one band (approximately 14 kDa) in all four cell lines (Fig. 2D), indicat-

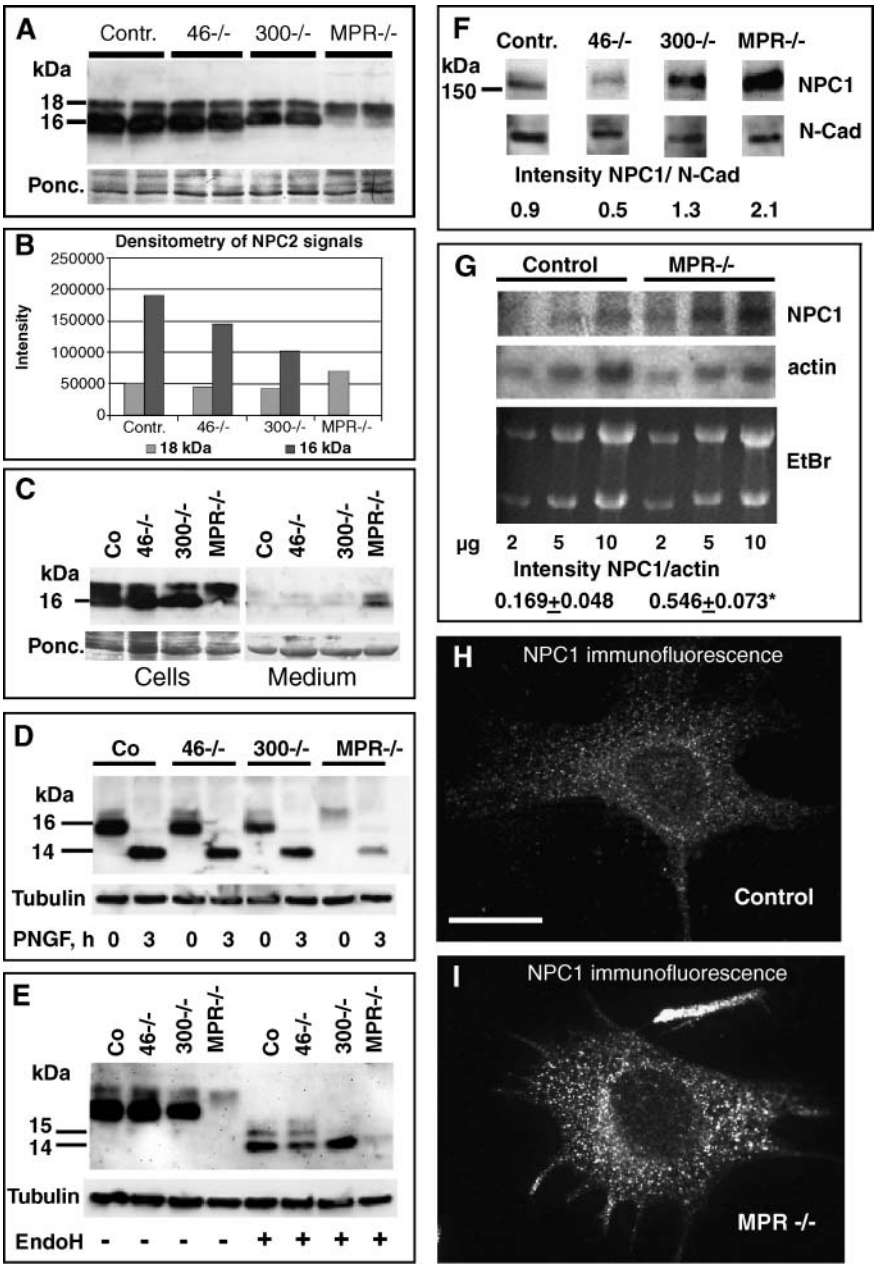


**Fig. 2.** Protein levels and glycosylation of NPC2 (A–E), and protein and mRNA levels of NPC1 (F–I), in wild-type cells (Contr.), MPR46$^{-/-}$ cells (46$^{-/-}$), MPR300$^{-/-}$ cells (300$^{-/-}$), and MPR46/MPR300$^{-/-}$ cells (MPR$^{-/-}$). A: Western blotting of endogenous NPC2. Equal amounts of protein were loaded on each lane. Ponceau staining (Ponc.) is shown as loading control. B: Quantitation of the bands shown in A. C: Western blotting of NPC2 in cell extracts and culture media. One day after seeding the cells on culture plates, the medium was replaced with DMEM containing 1% fetal calf serum. Four hours later, the medium and cells were harvested. Protein content of cell extracts was measured, and the volumes of culture media loaded to the gel were adjusted to correspond to equal amounts of cell protein for each cell line. Note that the lanes of cell extracts in C are overexposed, because longer exposure was necessary to detect NPC2 in the culture media. Ponceau staining is shown as loading control. D: Western blotting of NPC2 after digestion with peptide *N*-glycosidase F (PNGF). The same blot was stained with anti-tubulin to show equal loading in each lane. E: Western blotting of NPC2 after digestion with endoglycosidase H. Tubulin staining of the same blot is shown as loading control. F: Western blotting of NPC1 protein in the four fibroblast lines. *N*-cadherin (N-Cad) immunostaining is shown as loading control. Quantitation of the signals as a ratio of NPC1 to *N*-cadherin is shown under the blots. Similar results were obtained in two independent experiments. G: Northern blotting of NPC1 mRNA and actin mRNA in control and MPR-double-deficient cells, with three parallel total RNA samples (2, 5, and 10 µg) (upper part of the panel). The lower part of the panel shows the ethidium bromide (EtBr)-stained gel as a control for the integrity of the RNA. The signals for NPC1 and actin were quantified, and the NPC1 signal was divided by the actin signal for each lane. The three lanes were averaged, and the final values are shown (NPC1/actin, mean ± SD). *Statistical significance with 2-tailed Student's *t*-test ($P = 0.00295$). H, I: Immunofluorescence staining of endogenous NPC1 in control and MPR-double-deficient cells. Bar = 10 µm.

ing that NPC2 was glycosylated and that the size of the polypeptide was the same in all four cell lines. In control cells, endo H treatment revealed that a large proportion of NPC2 was endo H-sensitive (Fig. 2E, the 14 kDa band), indicating that the attached oligosaccharides were of high-mannose or hybrid type. In addition, we observed two endo H-resistant forms, a 15 kDa band and an additional faint band at 15–16 kDa. The oligosaccharides of these two forms are probably partially sensitive to endo H. These data indicate that all the oligosaccharides are endo H sensitive in some forms of NPC2, while other forms contain a mixture of endo H-sensitive and -resistant oligosaccharides. The bands observed in MPR46$^{-/-}$ cells were similar to those in control cells, suggesting that deficiency of MPR46 does not affect the glycosylation pattern of NPC2. In MPR300$^{-/-}$ cells, the resistant 15–16 kDa and 15 kDa bands were missing, and only the endo H-sensitive 14 kDa band was detectable. This indicates increased endo H sensitivity, and thus a decreased amount of complex carbohydrates, of NPC2 in MPR300-deficient cells. No endo H-resistant NPC2 (15–16 kDa or 15 kDa) was observed in MPR-double-deficient cells, indicating that in these cells also, all intracellular NPC2 was sensitive for endo H. The results indicate that the presence of MPRs affects the glycosylation pattern of NPC2. MPR300 seems to be particularly important for the formation of endo H-resistant complex oligosaccharide chains. The absence of complex carbohydrates could explain the slightly shifted molecular mass of the NPC2 main band observed in Western blots (Fig. 2A). It is possible that these complex oligosaccharide chains render NPC2 more resistant to the lysosomal hydrolytic enzymes.

### NPC1 expression is upregulated in MPR-double-deficient fibroblasts

The NPC1 and NPC2 proteins have been suggested to function at two different steps of the same pathway that transports cholesterol and other lipids out of late endosomes and/or lysosomes (1). We therefore also checked the expression levels of NPC1 protein in our four cell lines. Western blotting of cell extracts indicated that although the levels of NPC1 in MPR46$^{-/-}$ cells seemed to be lower than those in control cells (0.6-fold those of the controls), in MPR300$^{-/-}$ cells, the NPC1 protein level was

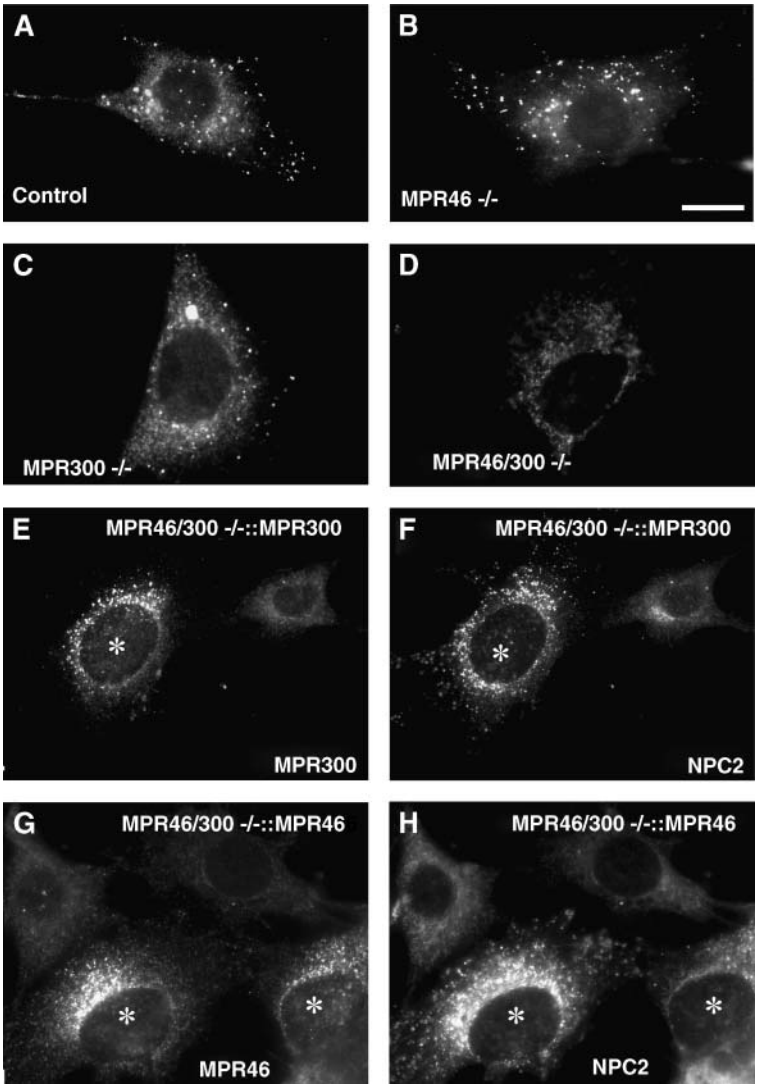


**Fig. 3.** Immunofluorescence staining of endogenous NPC2 in mouse embryonic fibroblast (MEF) cell lines. A–D: nontreated cells. The MPR-double-deficient cells in E–H were transiently transfected with a plasmid encoding human MPR300 (E, F) or human MPR46 (G, H), cultured for four days, and double stained for MPR300 (E) or MPR46 (G), and endogenous NPC2 (F, H). Asterisks indicate cells reexpressing MPR300 or MPR46. Note that the reexpression of either MPR restores the endo/lysosomal staining pattern of NPC2. Bar = 10 μm.

slightly higher than in control cells (1.4-fold those of the controls). MPR-double-deficient cells contained 2.3-fold higher levels of NPC1 protein than the control cells (Fig. 2F). This suggests that the cells try to compensate for the loss of NPC2 targeting by increasing the synthesis of NPC1. To investigate this, we performed Northern blotting to compare the mRNA levels. The signals of NPC1 mRNA were 3.2-fold more intense in the MPR-double-deficient cells, compared with those of the control cells (Fig. 2G). This confirmed that the higher NPC1 protein level was caused at least partially by an upregulation of transcription, and thus by increased protein synthesis. We also checked the subcellular localization of NPC1 in control and MPR-double-deficient cells by immunofluorescence staining. Both cell types showed a similar distribution in small cytoplasmic vesicles (Fig. 2H, I). The staining was, however, more intense in the MPR-double-deficient cells, which is in agreement with the Western and Northern blotting results.

### No lysosomal NPC2 can be detected in MPR-double-deficient fibroblasts

To investigate the subcellular localization of NPC2 in our cell lines, we performed immunofluorescence labeling. We used Bouin's fixation, which is necessary for detection of endogenous NPC2 (10). In control and MPR46$^{-/-}$ cells, NPC2 was detected in small, bright vesicles scattered around the cytoplasm (**Fig. 3A**, **B**). Bright vesicles were also detected in MPR300$^{-/-}$ cells (Fig. 3C), but their average number per cell seemed to be slightly reduced compared with the control cells. In addition to the vesicular staining, a faint reticular staining was observed around the nucleus (Fig. 3C). In contrast, no or only a very small amount of vesicular NPC2 staining was observed in the MPR-double-deficient cells. Only faint reticular staining was detected (Fig. 3D). To confirm that the lack of MPRs was the cause of NPC2 mislocalization, we performed a rescue experiment. MPR-double-deficient cells were transiently transfected with a plasmid encoding human MPR300 or human MPR46 and grown for four days. The cells were then fixed and double-stained for human MPR300 or MPR46 to detect the reexpressing cells and endogenous NPC2. In cells reexpressing MPR300 or MPR46, the endo/lysosomal pattern of NPC2 labeling was rescued. In contrast to the predominantly dispersed pattern of NPC2 staining in control and MPR46$^{-/-}$ cells (Fig. 3A, B), the NPC2 vesicles were more concentrated in the perinuclear region in the rescued cells, although dispersed vesicles were also observed (Fig. 3F, H).

Double labeling with the lysosomal membrane protein LAMP-1 revealed that the bright NPC2 vesicles observed

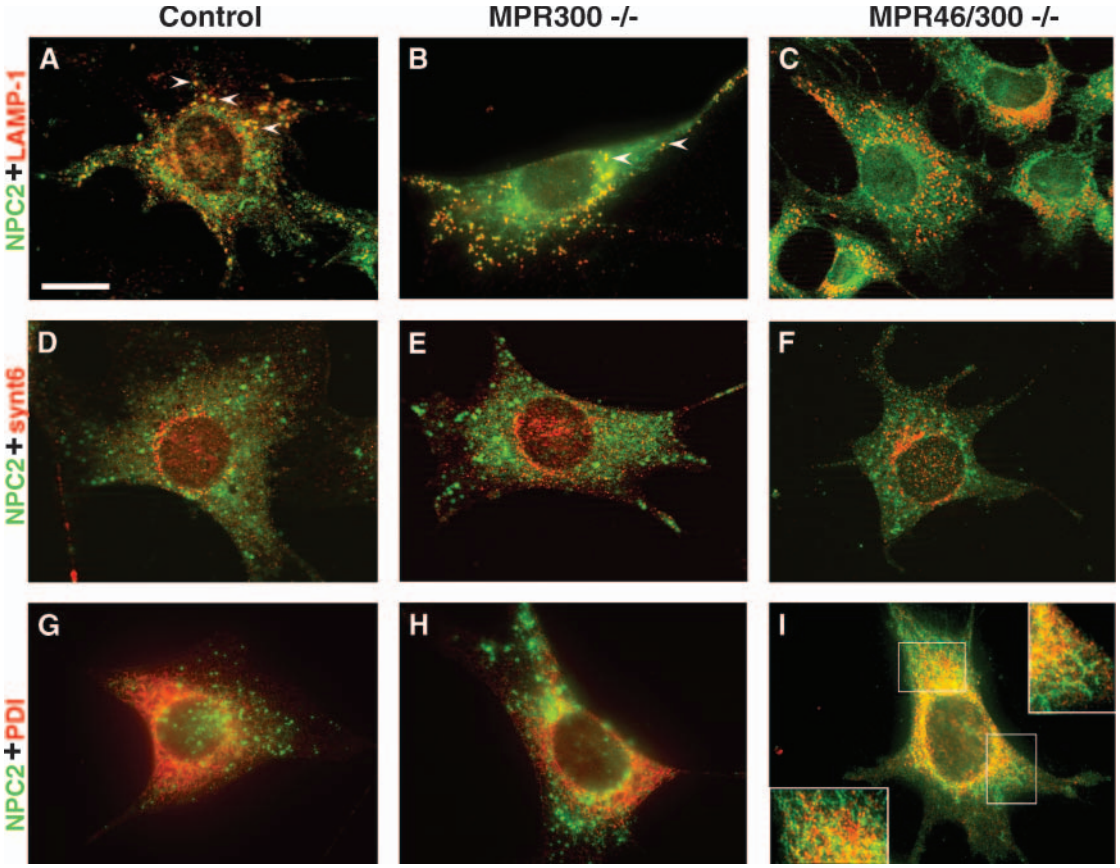


**Fig. 4.** Subcellular localization of endogenous NPC2 in control cells, MPR300$^{-/-}$ cells, and in MPR-double-deficient cells. Double labeling of NPC2 (green) with the lysosomal membrane protein LAMP-1 (red, upper row), the trans Golgi network marker protein syntaxin 6 (red, middle row), and the endoplasmic reticulum enzyme protein disulphide isomerase (PDI, red, lower row) are shown. Optical sections were obtained using the Apotome. Yellow color (arrowheads) indicates colocalization of the two labels. Bar = 10 μm.

in control cells were LAMP-1-positive, i.e., late endosomes or lysosomes (**Fig. 4A**). Colocalization of NPC2 and LAMP-1 was also detected in MPR46$^{-/-}$ cells (not shown) and in MPR300$^{-/-}$ cells (Fig. 4B). No colocalization of LAMP-1 and NPC2 was detected in the MPR-double-deficient cells (Fig. 4C), indicating that NPC2 was not targeted to the lysosomal compartment in these cells. This confirms our Western blotting results (Fig. 2A–C) and the suggestion that NPC2 is targeted to lysosomes by both MPRs. Very little colocalization of the TGN marker syntaxin 6 (27) with NPC2 was observed in any of the tested cell lines (Fig. 4D–F), indicating that in fibroblasts, NPC2 was not accumulating in the TGN. However, a limited colocalization of the ER marker, protein disulphide isomerase, and NPC2 was observed in the MPR-double-deficient cells (Fig. 4I), but not or much less so in control or MPR300$^{-/-}$ cells (Fig. 4G, H). This is in agreement with the defective lysosomal targeting of NPC2 in the MPR-double-deficient cells. The increased localization of NPC2 in the ER could be due to increased synthesis of NPC2 to compensate for the deficiency of NPC2 in lysosomes. Alternatively, there might be a decrease in the kinetics of trafficking out of the ER and Golgi complex due to the lack of MPRs. To differentiate between these alternatives, we performed Northern blotting of NPC2 mRNA. This revealed no difference between the control cells and MPR-double-deficient cells (not shown), suggesting that the increased ER localization of NPC2 in the double-deficient cells was due to retarded trafficking out of the ER. Taken together, immunofluorescence data indicate that in control cells and MPR46 (not shown) or MPR300-single-deficient cells, NPC2 is targeted to LAMP-1-positive endo/lysosomes, whereas no endo/lysosomal NPC2 could be detected in MPR-double-deficient cells.

### Unesterified cholesterol accumulates in endo/lysosomes of MPR-double-deficient cells

Mutations in or lack of NPC2 protein are known to cause accumulation of unesterified cholesterol in late-endosomal or -lysosomal compartments. To check whether unesterified cholesterol accumulated in any of the MPR-deficient cell lines, we used cholesterol labeling with filipin. In control cells, we observed staining on the plasma membrane and in vesicular-reticular structures in the perinuclear area (**Fig. 5A**), as expected in normal fibroblasts (21). In contrast, MPR-double-deficient cells showed bright staining in vesicles located predominantly in the perinu-

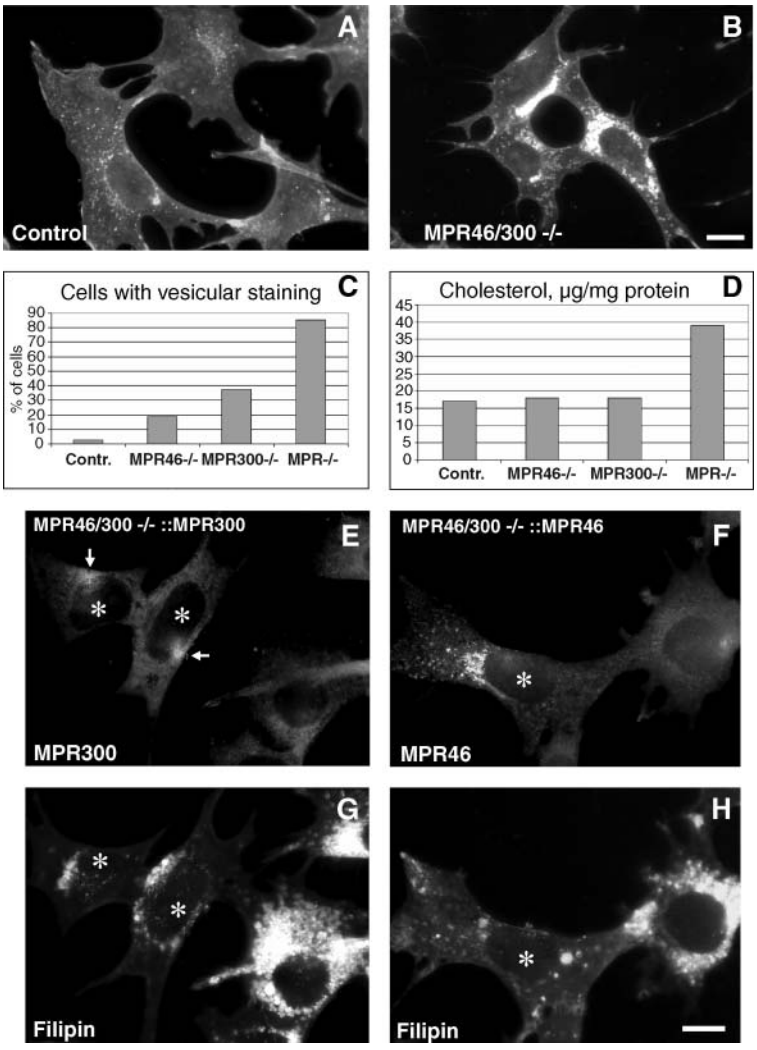


**Fig. 5.** Accumulation of unesterified cholesterol in MEFs deficient in both MPRs. Filipin staining of unesterified cholesterol in control cells (A) and MPR-double-deficient cells (B). Note the accumulation of bright vesicles in the perinuclear region in the MPR-double-deficient cells (B). C: Quantitation of filipin staining patterns in control MEFs and in MEFs deficient in MPR46, MPR300, or both MPRs (MPR$^{-/-}$). The percentage of cells showing accumulation of vesicular filipin staining as demonstrated in panel B is shown. D: Biochemical cholesterol assay in the four MEF cell lines. This assay detects both unesterified and esterified cholesterol. E–H: Reexpression of MPR300 or MPR46 can abolish the vesicular cholesterol accumulation. Fibroblasts deficient in MPR46 and MPR300 were transiently transfected with MPR300 (E, G) or MPR46 (F, H) and grown for two days. The reexpressing cells were identified by immunofluorescence staining of MPR300 (E) or MPR46 (F). Cholesterol was detected with filipin (G, H) in the same samples. Asterisks indicate the reexpressing cells. Note that filipin treatment is detrimental to the labeling pattern of MPR300; instead of the normal vesicular-reticular staining pattern (Fig. 1), in filipin-treated cells, MPR300 is located in one bright spot close to the nucleus (arrows in E). Bars = 10 μm.

clear area but also in the peripheral cytoplasm (Fig. 5B). Quantitation of labeling patterns (Fig. 5C) showed that more than 80% of the MPR-double-deficient cells had vesicular cholesterol accumulation (as demonstrated in Fig. 5B), whereas such staining was observed in less than 5% of control cells (Fig. 5C). MPR-single-deficient cells had an intermediate phenotype; approximately 20% of MPR46$^{-/-}$ cells and 38% of MPR300$^{-/-}$ cells showed vesicular cholesterol accumulation (Fig. 5C). This indicates that both MPRs are necessary for maximally efficient cholesterol trafficking, which in this case probably depends on lysosomal targeting of NPC2. However, either MPR alone is able to mediate enough NPC2 targeting to ameliorate the cholesterol accumulation to a substantial degree. Again, the defect was slightly more prominent in MPR300$^{-/-}$ cells, suggesting that this receptor is more efficient in NPC2 targeting than MPR46.

To confirm the microscopic results, we also performed a biochemical cholesterol assay that detects total, i.e., both unesterified and esterified, cholesterol. The total cholesterol levels of the MPR-single-deficient cell lines were similar to those of control cells, whereas the MPR-double-deficient cells had more than twice as much total cholesterol per cell protein (Fig. 5D). This result suggests that although the distribution of unesterified cholesterol was already slightly changed in the single-deficient cell lines (Fig. 5C), total cholesterol levels were comparable to those of control cells. However, in the double-deficient cells, both unesterified cholesterol distribution and total cholesterol amount were severely altered.

To further confirm the role of each MPR in cholesterol homeostasis, we performed rescue experiments by reexpressing MPR300 or MPR46 in the MPR-double-deficient cells. The cells were transfected with MPR46 or MPR300, grown for two days, and stained with anti-MPR antibodies to detect reexpressing cells (Fig. 5E, F) and with filipin to detect cholesterol (Fig. 5G, H). Transient reexpression of MPR300 or MPR46 was able to reduce the vesicular cholesterol accumulation to the control-cell level (Fig. 5E–H). These results indicate that the absence of MPRs was the primary reason for cholesterol accumulation in the MPR-double-knockout cells.

NPC disease fibroblasts accumulate glycolipids and other lipids, including bis(monoacylglycero)phosphate (BMP), in addition to cholesterol. We therefore tested whether the MPR-double-deficient cells also show this phenotype. Immunofluorescence staining with anti-BMP revealed a moderate accumulation of vesicular staining in the MPR-double-deficient cells (**Fig. 6**, upper row). Labeling with cholera toxin to detect GM1 showed a mild accumulation of perinuclear vesicular staining in the MPR-double-knockout cells (Fig. 6, middle row), whereas no accumulation was observed with anti-GM2 antibody staining (Fig. 6, lower row). We also performed TLC of extracted lipids under conditions that separate sphingomyelin, cerebroside, glucocerebroside, and phosphatidic acid, as well as phosphatidylcholine, -inositide, -serine, and -ethanolamine. This analysis revealed no differences between the control cells and MPR-double-deficient cells (not shown). These results indicate that the MPR-double-deficient cells accumulate, in

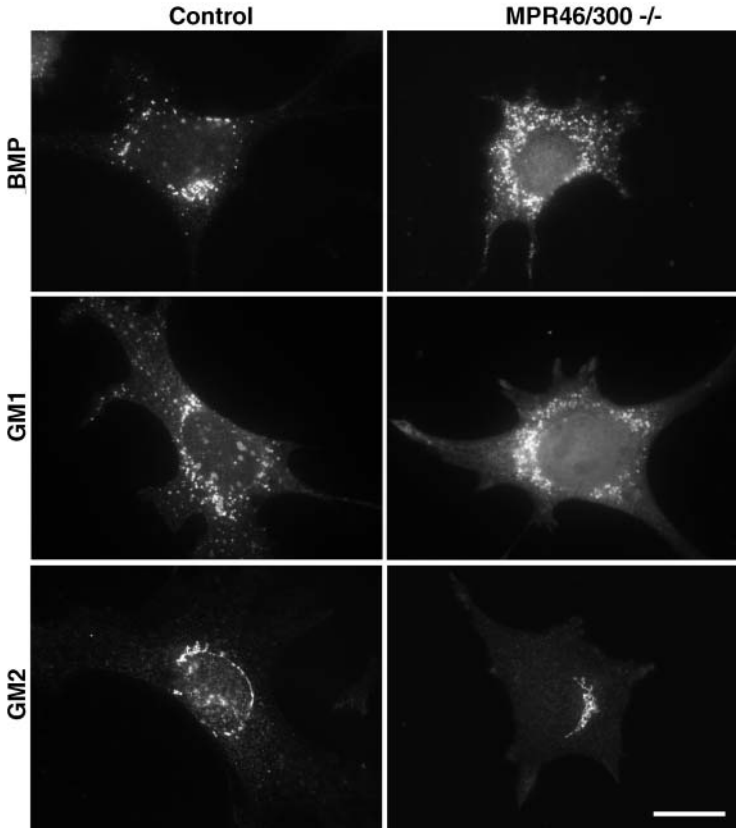


**Fig. 6.** Lipid localization in control and MPR-double-deficient cells. The cells were fixed and stained with anti-bis (monoacylglycero)phosphate (BMP), cholera toxin to detect the ganglioside GM1, or anti-GM2 as indicated. Bar = 10 μm.

addition to cholesterol, moderate amounts of BMP (but no phosphatidic acid), only low levels of the ganglioside GM1, but no GM2, cerebroside, sphingomyelin, or other phospholipids.

To investigate the nature of the filipin-positive vesicles accumulating in the MPR-double-deficient cells, we performed immunofluorescence labeling. In NPC1 and NPC2 patient fibroblasts (28) and LAMP-1/LAMP-2-double-deficient fibroblasts (21), cholesterol accumulates in late-endosomal vesicles. We therefore tested whether late-endosomal markers colocalize with the filipin-positive vesicles in the MPR-double-deficient cells. To study colocalization with the late-endosomal small GTPase Rab7, we transiently transfected the cells with GFP-Rab7. We observed some colocalization of Rab7 and filipin staining in control cells (**Fig. 7A**), whereas in MPR-double-deficient cells, the two labels overlapped more extensively (Fig. 7B). Rab7 was particularly concentrated in the limiting membrane of vesicles that showed filipin staining in their lumen (Fig. 7B, inserts). A similar result was obtained by immunofluorescence staining of the lysosomal membrane protein LAMP-1 (Fig. 7C, D). These findings indicate that in the MPR-double-deficient fibroblasts, unesterified cholesterol accumulated in late-endosomal/lysosomal vesicles. This result is consistent with the suggestion that the lack of endo/lysosomal NPC2 directly or indirectly caused the accumulation of cholesterol.

To further characterize the compartment that accumulates cholesterol in the MPR-double-deficient cells, we also performed transmission electron microscopy of filipin-labeled cells. Membrane-associated cholesterol can be detected in transmission electron microscopy using filipin, which induces typical folding to cholesterol-rich membranes. We have shown previously that in wild-type fibroblasts, the perinuclear filipin staining corresponds to small vesicles that typically localize close to the Golgi apparatus (21). An identical filipin labeling pattern was observed in the control cells (**Fig. 8A**, **A′**). In MPR-double-deficient cells, we observed an accumulation of very characteristic, electron-dense, approximately 1 μm-diameter vesicles that contained small internal vesicles and amorphous material (Fig. 8B). The morphology of these multivesicular structures corresponded to late-endosome morphology (29). High magnification revealed that the limiting membranes of these structures were heavily labeled by filipin (Fig. 8B, B′), indicating that they were the sites of cholesterol accumulation in the MPR-double-deficient cells. The electron microscope analysis thus confirmed the late-endosomal nature of the cholesterol-accumulating organelles.

## DISCUSSION

### Subcellular localization of NPC2

The subcellular localization of NPC2 protein has been studied using cell fractionation and immunofluorescence techniques. Endogenous rat liver NPC2 was shown to cofractionate with lysosomal enzyme activities (4). By immunofluorescence, endogenous NPC2 of human fibroblasts was shown to localize in LAMP-1-positive and LAMP-1-negative vesicles as well as in the TGN (30), or in cathepsin D-positive vesicles (10). Furthermore, endocytosed NPC2-red fluorescent protein was shown to localize in the lumen of vesicles that contained NPC1-green fluorescent protein in their periphery (10). However, it has been shown that only very little colocalization can be observed between endogenous NPC1 and NPC2 (15). In the present study, we observed that endogenous NPC2 in MEFs localized to LAMP-1-positive vesicles. In addition, we could not detect colocalization of NPC2 with syntaxin 6, a TGN marker (27), or protein disulphide isomerase, an ER marker. Taken together, these results indicate that endogenous NPC2 localizes to LAMP-1- and cathepsin D-positive vesicles, i.e., late endosomes and/or lysosomes. In some cell types, NPC2 may also be detected in the TGN. This is in agree-

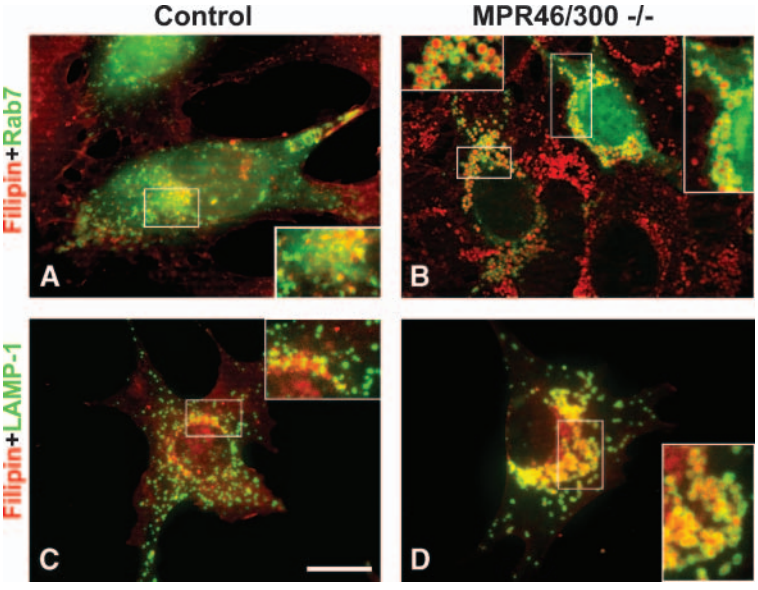


**Fig. 7.** Cholesterol accumulates in late endosomal/lysosomal vesicles in the MPR-double-deficient cells. A, B: Control and MPR-double-deficient cells were transiently transfected with GFP-Rab7 (green). Filipin staining is shown in red. Two cells expressing Rab7 are shown in B; the one on the left is expressing a lower level than the one on the right. Note that in the double-deficient cells, Rab7 localizes in the limiting membranes of cholesterol-loaded vesicles (inserts in panel B). C, D: Control and MPR-double-deficient cells were labeled with filipin (red) and anti-LAMP-1 antibodies (green). Similar to Rab7, LAMP-1 localizes in the limiting membranes of cholesterol-loaded vesicles (insert in D). Bar = 10 μm.

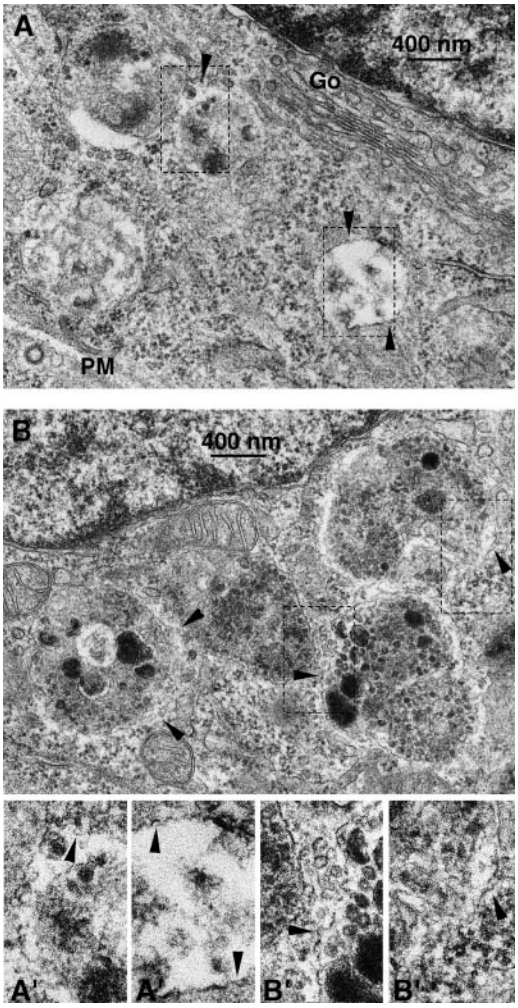


**Fig. 8.** Transmission electron microscopy of filipin-labeled control (A) and MPR-double-deficient (B) cells. Filipin labeling is seen as folding of the cholesterol-rich membrane (arrowheads in A′, B′). Go, Golgi apparatus; PM, plasma membrane. B: Electron-dense multivesicular structures characteristic of the MPR-double-deficient cells. The membranes of these structures were heavily labeled by filipin (arrowheads in B′).

ment with the localization of other soluble lysosomal proteins such as cathepsin D and cathepsin L (E-L. Eskelinen, unpublished observations). Because endogenous NPC1 and NPC2 do not colocalize (see above), it is possible that NPC1 is located in the subset of late endosomes that do not contain NPC2. However, after cholesterol loading, NPC1 seems to be recruited to the cholesterol-containing compartments (3), i.e., the same compartments that contain NPC2. It has been proposed that NPC2 assists in cholesterol transport out of late endosomes/lysosomes, possibly by transporting cholesterol from the internal membranes to the limiting membrane, where NPC1 could bind it and assist its transfer to a cytoplasmic acceptor (31). In this context, it is surprising that the subcellular distribution of NPC1 protein was not altered in the MPR-double-deficient cells (Fig. 2H, I), although these cells showed a prominent accumulation of cholesterol in enlarged late-endosomal compartments (Figs. 5, 7). It is conceivable that NPC2 function would be needed for the recruitment of NPC1 to the cholesterol-loaded late endosomes.

### NPC2 needs MPRs for correct intracellular targeting in fibroblasts

In the paper in which it was originally reported that *HE1/NPC2* is the second gene in NPC disease, it was also observed that cholesterol accumulation of NPC2-deficient cells could be reduced by adding NPC2 to the culture medium. It was further observed that simultaneous addition of mannose 6-phosphate to the medium prevented this rescue effect (4). It has also been shown that, similar to NPC patient cells, inclusion cells (I-cells) accumulate unesterified cholesterol in their endo/lysosomal compartments (15). In I-cell disease, mutations in the phosphotransferase gene prevent the addition of mannose 6-phosphate tags to all soluble MPR-dependent lysosomal proteins, which include NPC2 (32). Indeed, addition of wild-type NPC2 protein to the culture medium of I-cells reduced the endo/lysosomal cholesterol accumulation (15), indicating that NPC2 protein is dependent on mannose 6-phosphate-mediated uptake and targeting. Our present results are in agreement with this model. Our findings indicate that MPRs are indeed needed for the proper intracellular targeting and function of the NPC2 protein. Further, our findings demonstrate that either MPR46 or MPR300 alone can transport NPC2 to the endo/lysosomal compartment, although MPR300 seems to be more efficient than MPR46. The lack of both MPRs leads to complete mistargeting of NPC2 to the culture medium, and to a massive accumulation of unesterified cholesterol in the endo/lysosomal compartment. Taken together, these results suggest that NPC2 disease could in future be treated using an enzyme replacement therapy approach similar to those used in other lysosomal storage diseases caused by mutations in genes encoding soluble lysosomal enzymes (33).

Using electron microscopy, we observed an accumulation of electron-dense multivesicular bodies in the MPR-double-deficient fibroblasts. Similar electron-dense multivesicular structures have been detected in cultured fibroblasts of I-cell patients (34). This shows that interference with mannose 6-phosphate-dependent targeting, either because of defects in the enzyme that adds the tag to the ligand proteins, or because of defects in the receptors, can lead to similar ultrastructural outcomes.

### NPC1 and NPC2 synthesis rates may be regulated in concert

It has been observed that the protein and mRNA levels of NPC2 are upregulated in NPC1 patient cells (30). In this paper, we show that the NPC1 protein and mRNA levels are upregulated in the MPR-double-deficient fibroblasts, which are deficient in NPC2 intracellular targeting. Together, these results support the idea that the synthesis rates of NPC1 and NPC2 may be regulated in concert; in other words, one can be upregulated in the attempt to compensate for the loss of the other. This supports the proposal that these two proteins act in the same lipid transport pathway (31).

## CONCLUSIONS

In this paper, we show that in fibroblasts, NPC2 protein needs MPR46 or MPR300, or both MPRs, for correct targeting to the endo/lysosomal compartment. These results show that the MPR-dependent targeting of NPC2 protein is very similar to that of soluble lysosomal enzymes. Our results support the idea that NPC2 disease could be treated using an enzyme replacement therapy approach similar to those used in other lysosomal storage diseases caused by mutations in genes encoding soluble lysosomal enzymes.

The authors are grateful to Marlies Rusch, Katharina Stiebeling, and Ellen Eckermann for technical assistance. The authors also thank William S. Garver, Shutish Patel, Stephen Fuller, Thomas Braulke, and Jean Gruenberg for reagents. This work was supported by the Deutche Forschungsgemeinschaft, the Hensel Stiftung, the Fonds der Chemischen Industrie, and the German National NPC Parents Organzation.

## REFERENCES

1. Vanier, M. T., and G. Millat. 2003. Niemann-Pick disease type C. *Clin. Genet.* **64:** 269–281.
2. Vanier, M. T., and G. Millat. 2004. Structure and function of the NPC2 protein. *Biochim. Biophys. Acta.* **1685:** 14–21.
3. Zhang, M., N. K. Dwyer, E. B. Neufeld, D. C. Love, A. Cooney, M. Comly, S. Patel, H. Watari, J. F. R. Strauss, P. G. Pentchev, et al. 2001. Sterol-modulated glycolipid sorting occurs in Niemann-Pick C1 late endosomes. *J. Biol. Chem.* **276:** 3417–3425.
4. Naureckiene, S., D. E. Sleat, H. Lackland, A. Fensom, M. T. Vanier, R. Wattiaux, M. Jadot, and P. Lobel. 2000. Identification of HE1 as the second gene of Niemann-Pick C disease. *Science.* **290:** 2298–2301.
5. Davies, J. P., F. W. Chen, and Y. A. Ioannou. 2000. Transmembrane molecular pump activity of Niemann-Pick C1 protein. *Science.* **290:** 2295–2298.
6. Ohgami, N., D. C. Ko, M. Thomas, M. P. Scott, C. C. Chang, and T. Y. Chang. 2004. Binding between the Niemann-Pick C1 protein and a photoactivatable cholesterol analog requires a functional sterol-sensing domain. *Proc. Natl. Acad. Sci. USA.* **101:** 12473–12478.
7. Ko, D. C., J. Binkley, A. Sidow, and M. P. Scott. 2003. The integrity of a cholesterol-binding pocket in Niemann-Pick C2 protein is necessary to control lysosome cholesterol levels. *Proc. Natl. Acad. Sci. USA.* **100:** 2518–2525.
8. Sleat, D. E., J. A. Wiseman, M. El-Banna, S. M. Price, L. Verot, M. M. Shen, G. S. Tint, M. T. Vanier, S. U. Walkley, and P. Lobel. 2004. Genetic evidence for nonredundant functional cooperativity between NPC1 and NPC2 in lipid transport. *Proc. Natl. Acad. Sci. USA.* **101:** 5886–5891.
9. Okamura, N., S. Kiuchi, M. Tamba, T. Kashima, S. Hiramoto, T. Baba, F. Dacheux, J. L. Dacheux, Y. Sugita, and Y. Z. Jin. 1999. A porcine homolog of the major secretory protein of human epididymis, HE1, specifically binds cholesterol. *Biochim. Biophys. Acta.* **1438:** 377–387.
10. Zhang, M., M. Sun, N. K. Dwyer, M. E. Comly, S. C. Patel, R. Sundaram, J. A. Hanover, and E. J. Blanchette-Mackie. 2003. Differential trafficking of the Niemann-Pick C1 and 2 proteins highlights distinct roles in late endocytic lipid trafficking. *Acta Paediatr. Suppl.* **443:** 63–73.
11. Storch, S., and T. Braulke. 2005. Transport of lysosomal enzymes. *In* Lysosomes. P. Saftig, editor. Landes Bioscience/Eurekah.com, Georgetown, TX. 18–27.
12. Kasper, D., F. Dittmer, K. von Figura, and R. Pohlmann. 1996. Neither type of mannose 6-phosphate receptor is sufficient for targeting of lysosomal enzymes along intracellular routes. *J. Cell Biol.* **134:** 615–623.
13. Munier-Lehmann, H., F. Mauxion, U. Bauer, P. Lobel, and B. Hoflack. 1996. Re-expression of the mannose 6-phosphate receptors in receptor-deficient fibroblasts. Complementary function of the two mannose 6-phosphate receptors in lysosomal enzyme targeting. *J. Biol. Chem.* **271:** 15166–15174.
14. Pohlmann, R., M. Wendland, C. Boeker, and K. von Figura. 1995. The two mannose 6-phosphate receptors transport distinct complements of lysosomal proteins. *J. Biol. Chem.* **270:** 27311–27318.
15. Chikh, K., S. Vey, C. Simonot, M. T. Vanier, and G. Millat. 2004. Niemann-Pick type C disease: importance of N-glycosylation sites for function and cellular location of the NPC2 protein. *Mol. Genet. Metab.* **83:** 220–230.
16. Klumperman, J., A. Hille, T. Veenendaal, V. Oorschot, W. Stoorvogel, K. von Figura, and H. J. Geuze. 1993. Differences in the endosomal distributions of the two mannose 6-phosphate receptors. *J. Cell Biol.* **121:** 997–1010.
17. Claussen, M., D. Buergisser, A. G. Schuller, U. Matzner, and T. Braulke. 1995. Regulation of insulin-like growth factor (IGF)-binding protein-6 and mannose 6-phosphate/IGF-II receptor expression in IGF-IL-overexpressing NIH 3T3 cells. *Mol. Endocrinol.* **9:** 902–912.
18. Breuer, P., C. Korner, C. Boker, A. Herzog, R. Pohlmann, and T. Braulke. 1997. Serine phosphorylation site of the 46-kDa mannose 6-phosphate receptor is required for transport to the plasma membrane in Madin-Darby canine kidney and mouse fibroblast cells. *Mol. Biol. Cell.* **8:** 567–576.
19. Körner, C., B. Nürnberg, M. Uhde, and T. Braulke. 1995. Mannose 6-phosphate/insulin-like growth factor II receptor fails to interact with G-proteins. *J. Biol. Chem.* **270:** 287–295.
20. Bucci, C., P. Thomsen, P. Nicoziani, J. McCarthy, and B. van Deurs. 2000. Rab7: a key to lysosome biogenesis. *Mol. Biol. Cell.* **11:** 467–480.
21. Eskelinen, E. L., C. K. Schmidt, S. Neu, M. Willenborg, G. Fuertes, N. Salvador, Y. Tanaka, R. Lüllmann-Rauch, D. Hartmann, J. Heeren, et al. 2004. Disturbed cholesterol traffic but normal proteolytic function in LAMP-1/LAMP-2 double-deficient fibroblasts. *Mol. Biol. Cell.* **15:** 3132–3145.
22. Isbrandt, D., G. Arlt, D. A. Brooks, J. J. Hopwood, K. von Figura, and C. Peters. 1994. Mucopolysaccharidosis VI (Maroteaux-Lamy syndrome): six unique arylsulfatase B gene alleles causing variable disease phenotypes. *Am. J. Hum. Genet.* **54:** 454–463.
23. Lehmann, L. E., W. Eberle, S. Krull, V. Prill, B. Schmidt, C. Sander, K. von Figura, and C. Peters. 1992. The internalization signal in the cytoplasmic tail of lysosomal acid phosphatase consists of the hexapeptide PGYRHV. *EMBO J.* **11:** 4391–4399.
24. Folch, J., M. Lees, and S. G. H. Sloane. 1957. A simple method for the isolation and purification of total lipids from animal tissues. *J. Biol. Chem.* **224:** 497–509.
25. Trimble, R. B., A. L. Tarentino, T. H. J. Plummer, and F. Maley. 1978. Asparaginyl glycopeptides with a low mannose content are hydrolyzed by endo-beta-N-acetylglucosaminidase H. *J. Biol. Chem.* **253:** 4508–4511.
26. Tarentino, A. L., C. M. Gomez, and T. H. J. Plummer. 1985. Deglycosylation of asparagine-linked glycans by peptide:N-glycosidase F. *Biochemistry.* **24:** 4665–4671.
27. Bock, J. B., J. Klumperman, S. Davanger, and R. H. Scheller. 1997. Syntaxin 6 functions in trans-Golgi network vesicle trafficking. *Mol. Biol. Cell.* **8:** 1261–1271.
28. Ikonen, E., and M. Hölttä-Vuori. 2004. Cellular pathology of Niemann-Pick type C disease. *Semin. Cell Dev. Biol.* **15:** 445–454.
29. Möbius, W., E. van Donselaar, Y. Ohno-Iwashita, Y. Shimada, H. F. G. Heijnen, J. W. Slot, and H. J. Geuze. 2003. Recycling compartments and the internal vesicles of multivesicular bodies harbor most of the cholesterol found in the endocytic pathway. *Traffic.* **4:** 222–231.
30. Blom, T. S., M. D. Linder, K. Snow, H. Pihko, M. W. Hess, E. Jokitalo, V. Veckman, A. C. Syvanen, and E. Ikonen. 2003. Defective endocytic trafficking of NPC1 and NPC2 underlying infantile Niemann-Pick type C disease. *Hum. Mol. Genet.* **12:** 257–272.
31. Storch, J., and S. R. Cheruku. 2005. Cholesterol transport in lysosomes. *In* Lysosomes. P. Saftig, editor. Landes Bioscience/Eurekah.com, Georgetown, TX. 102–113.
32. Holzman, E. 1989. Lysosomes. Plenum Press, New York, NY.
33. Matzner, U. 2005. Therapy of lysosomal storage diseases. *In* Lysosomes. P. Saftig, editor. Landes Bioscience/Eurekah.com, Georgetown, TX. 114–131.
34. Brown, W. J., and M. G. Farquhar. 1984. Accumulation of coated vesicles bearing mannose 6-phosphate receptors for lysosomal enzymes in the Golgi region of I-cell fibroblasts. *Proc. Natl. Acad. Sci. USA.* **81:** 5135–5139.